

MHD Sausage Mode Oscillations in Coronal Loops

Markus J. Aschwanden¹, Valery M. Nakariakov², and Victor F. Melnikov³

ABSTRACT

A recent study by Nakariakov et al. pointed out that the dispersion relation of MHD sausage mode oscillations has been incorrectly applied to coronal loops, neglecting the highly dispersive nature of the phase speed and the long-wavelength cutoff of the wave number. In the light of these new insights we revisit previous observations that have been interpreted in terms of MHD sausage mode oscillations in coronal loops and come to the following conclusions: (1) Fast sausage MHD mode oscillations require such a high electron density imposed by the wave number cutoff that they can only occur in flare loops; (2) In the previously reported radio observations ($\nu \approx 100$ MHz to 1 GHz) with periods of $P \approx 0.5 - 5$ s, the fast sausage MHD mode oscillation is likely to be confined to a small segment (corresponding to a high harmonic node) near the apex of the loop, rather than involving a global oscillation over the entire loop length. The recent microwave and soft X-ray observations of fast periods ($P \approx 6 - 17$ s) by Asai et al. and Melnikov et al., however, are consistent with fast sausage MHD oscillations at the fundamental harmonic.

Subject headings: Sun: Corona — Sun: UV radiation

1. INTRODUCTION

Coronal seismology became an efficient new tool that uses standing MHD waves and oscillations as a tool to explore the physical parameters of the solar corona. There are three basic branches of solutions of the dispersion relation for propagating and standing MHD waves: the slow mode branch (with acoustic phase speeds), the fast mode branch and the Alfvén branch (with Alfvénic phase speeds). Furthermore, each branch has a symmetric and asymmetric solution, termed the sausage and kink mode (Roberts et al. 1984). All of these MHD oscillation modes have been now detected with imaging observations in recent years: transverse fast kink-mode oscillations with TRACE (Aschwanden et al. 1999; Nakariakov et al. 1999); longitudinal (slow-magnetoacoustic) modes with SUMER (Wang et al. 2002; Ofman & Wang 2002), and fast sausage-mode oscillations probably with the *Nobeyama Radioheliograph* (Asai et al. 2001; Melnikov, Reznikova, & Shibasaki 2002). The latter type of fast sausage-mode oscillations is the least established one, although numerous non-imaging radio observations exist that have been interpreted earlier in terms of this mode. However, a recent study by Nakariakov et al. (2003) pointed out that the dispersion

¹Lockheed Martin Advanced Technology Center, Solar & Astrophysics Laboratory, Dept. L9-41, Bldg.252, 3251 Hanover St., Palo Alto, CA 94304, USA; e-mail: aschwanden@lmsal.com

²Physics Department, University of Warwick, Coventry, CV4 7AL, United Kingdom; valery@astro.warwick.ac.uk

³Radiophysical Research Institute (NIRFI), 25 Bol'shaya Pecherskaya, Nizhny Novgorod 603950, Russia

relation and oscillation period has been incorrectly applied to the data, because the highly dispersive nature of the phase speed and the long-wavelength cutoff in the wave number has been ignored. Here we revisit the relevant earlier radio observations in the light of these new insights and attempt to derive the correct physical parameters.

2. THEORY

The dispersion relation for magnetosonic waves in cylindrical magnetic flux tubes has infinitely many types of long-wavelength solutions in the fast-mode branch ($n = 0, 1, 2, 3, \dots$), with the lowest ones called sausage modes ($n = 0$) and kink modes ($n = 1$). The solutions are depicted in Fig. 1, showing that the kink mode solution extends all the way to the long-wavelength limit $ka \mapsto 0$, while the sausage mode has a cutoff at a phase speed of $v_{ph} = v_{Ae}$, which has no solution for small wave numbers $ka < k_c a$. The propagation cutoff for the sausage mode occurs at the cutoff wave number k_c (Edwin & Roberts 1983; Roberts et al. 1984),

$$k = k_c = \left[\frac{(c_s^2 + v_A^2)(v_{Ae}^2 - c_T^2)}{(v_{Ae}^2 - v_A^2)(v_{Ae}^2 - c_s^2)} \right]^{1/2} \left(\frac{j_{0,s}}{a} \right), \quad s = 1, 2, 3, \dots \quad (1)$$

where $j_{0,s} = (2.40, 5.52, \dots)$ are the zeros of the Bessel function J_0 . Here we restrict our attention to the genuine sausage mode with transverse mode number $s = 1$, i.e. $j_{0,1}$. The cutoff frequency ω at the cutoff is $k_c v_{Ae} = \omega_c$. Under coronal conditions, the sound speed amounts typically to $c_s = 150 \times \sqrt{T_{MK}} \approx 150 - 260$ km s⁻¹ (with $T \approx 1 - 3$ MK), which is much smaller than the typical Alfvén speed ($v_A \approx 1000$ km s⁻¹) so we have $c_s \ll v_A$. In this case the tube speed,

$$c_T = \frac{c_s^2 v_A^2}{(c_s^2 + v_A^2)}, \quad (2)$$

is similar to the sound speed, $c_T \lesssim c_s$, and the expression for the cutoff wave number k_c (Eq. 1) simplifies to,

$$k_c \approx \left(\frac{j_{0,s}}{a} \right) \left[\frac{1}{(v_{Ae}/v_A)^2 - 1} \right]^{1/2} \quad (3)$$

In the low- β corona, the thermal pressure is much smaller than the magnetic pressure, so that we can assume almost identical magnetic field strengths inside and outside of coronal loops, i.e., $B_0 \approx B_e$, so that the ratio of external to the internal Alfvén speed v_{Ae}/v_A is essentially a density ratio $\sqrt{n_0/n_e}$,

$$k_c \approx \left(\frac{j_{0,s}}{a} \right) \left[\frac{1}{n_0/n_e - 1} \right]^{1/2} \quad (4)$$

From this expression we see that for typical density ratios inferred in the solar corona, e.g., $n_e/n_0 \approx 0.1 - 0.5$ (Aschwanden et al. 2003), the cutoff wave number $k_c a$ falls into the range of $0.8 \lesssim k_c a \lesssim 2.4$. Therefore, we would expect that a long-wavelength sausage mode oscillation is completely suppressed for the slender loops for which kink mode oscillations have been observed, which have wave numbers of $ka = 2\pi a/\lambda = (\pi/2)(w/l) \approx 0.04 - 0.08$ (Aschwanden et al. 2002). Coronal conditions with $ka \ll 1$ were also inferred from fast kink mode oscillations (Nakariakov & Ofman 2001). Of course, higher harmonics would have correspondingly shorter wavelengths, i.e. $k = N\pi/l$ with $N = 1, 2, 3, \dots$. On the other side, the short-wavelength limit is given by the maximum possible loop width ($a = w/2 \leq l$), so the maximum wave number is $ka \leq k_m a = 2\pi(a/\lambda)_m = \pi(a/l)_m = \pi$. The occurrence of global sausage mode

oscillations therefore requires special conditions, $k_c < k < k_m$, i.e., very high density contrast n_0/n_e and relatively thick loops to satisfy $k > k_c$. The high density ratio, i.e., $n_0/n_e \gg 1$ or $v_{Ae} \gg v_A$, yields the following simple expressions for the cutoff wave number k_c ,

$$k_c a \approx j_{0,s} \left(\frac{v_A}{v_{Ae}} \right) = j_{0,s} \left(\frac{n_e}{n_0} \right)^{1/2} \quad (5)$$

Since the wavelength of the fundamental eigenmode (with harmonic number $N = 1$ in longitudinal direction and mode number $s = 1$ in transverse direction) corresponds to the double loop length, so that the wavenumber relates to the loop length by $k = 2\pi/\lambda = \pi/l$, the cutoff wave number condition $k > k_c$ implies a constraint between the loop geometry ratio w/l and the density contrast n_e/n_0 ,

$$\frac{l}{w} = \frac{\pi}{2ak} < \frac{\pi}{2ak_c} = \frac{\pi}{2j_{0,s}} \sqrt{\frac{n_0}{n_e}} \approx 0.65 \sqrt{\frac{n_0}{n_e}} , \quad (6)$$

The numerical factor 0.65 applies to the fundamental ($s = 1$) sausage mode. Since geometric parameters (such as l and w) can be measured easier than densities, we might turn the cutoff condition around and formulate it as a density contrast requirement for a given loop aspect ratio,

$$\frac{n_0}{n_e} > \left(\frac{1}{0.65} \frac{l}{w} \right)^2 = 2.4 \left(\frac{l}{w} \right)^2 . \quad (7)$$

This clearly indicates that slender loops with a high length-to-width ratio $l/w \gg 1$ would require extremely high density contrast n_0/n_e . Typical active region loops, which have only a moderate density contrast in the order of $n_0/n_e \approx 2 - 10$, would be required to be extremely fat, with width-to-length ratios of $l/w \approx 1 - 2$. The density contrast is much higher for flare loops or postflare loops, up to $n_0/n_e \approx 10^2, \dots 10^3$. In this case, a length-to-width ratio of $l/w \approx 6 - 20$ would be allowed for sausage mode oscillations. This brings us to the conclusion that global sausage type oscillations are only expected in fat and dense loops, basically only in flare and postflare loops, a prediction that was not appreciated until recently (Nakariakov et al. 2003). The restriction of the sausage mode wave number cutoff is visualized in Fig. 2, where the permitted range of geometric loop aspect ratios (l/w) is shown as function of the density contrast (n_0/n_e).

Since the sausage mode is highly dispersive in the long-wavelength part of the spectrum (see Fig. 1), the phase speed v_{ph} is a strong function of the wavenumber ka . The phase speed diagram Fig. 1 shows that the phase speed equals to the external Alfvén speed at the long-wavelength cutoff, $v_{ph}(k = k_c) = v_{Ae}$, and tends to approach the internal Alfvén speed in the short-wavelength limit, $v_{ph}(ka \gg 1) \mapsto v_A$. For coronal conditions, the phase speed of both the fast kink and fast sausage mode are bound by the internal and external Alfvén velocities,

$$v_A \leq v_{ph} = \frac{\omega}{k} \leq v_{Ae} , \quad (8)$$

Therefore, also the period ($P = 2l/v_{ph}$) of the standing sausage mode is bound by these two limits,

$$\frac{2l}{v_{Ae}} < P_{saus} = \frac{2l}{v_{ph}} < \frac{2l}{v_A} . \quad (9)$$

At the lower limit we can derive a simple relation for the sausage mode period from the long-wavelength cutoff, where $v_{ph}(k = k_c) = v_{Ae}$, using Eq. 6,

$$P_{saus} = \frac{2l}{v_{ph}} = \frac{2\pi}{kv_{ph}(k)} < \frac{2\pi}{k_c v_{ph}(k_c)} \approx \frac{2\pi a}{j_{0,s} v_{Ae}} \left(\frac{v_{Ae}}{v_A} \right) = \frac{2\pi a}{j_{0,s} v_A} = \frac{2.62 a}{v_A} . \quad (10)$$

an approximation that is also derived in Rosenberg (1970) and Roberts et al. (1984). However, one should be aware that this relation represents only a lower limit that applies at $k = k_c$, while for all other valid wavenumbers ($k > k_c$) the loop length is shorter ($l = \pi/k$) and thus the global sausage mode period P_{saus} is also shorter (Nakariakov et al. 2003), given by the actual phase speed $v_{ph}(k = \pi/l)$ defined by the dispersion relation (Fig. 1) at a particular value $k > k_c$,

$$P_{saus}(l) = \frac{2l}{v_{ph}(k = \pi/l)} , \quad (11)$$

Provided that sufficiently fat and overdense loops exist according to the requirement (Eq. 6 or 7), we expect for a loops radius of $a \approx 1000$ km and an Alfvén speed of $v_A \approx 1000$ km s⁻¹ a typical sausage mode period of $P_{saus} \leq 2.6$ s (according to Eq. 10).

3. OBSERVATIONS

Table 1 contains a compilation of radio observations of oscillation events with periods in the range of $0.5 \text{ s} < P < 1 \text{ min}$. Most of these observations have been interpreted in terms of MHD fast sausage mode oscillations, mainly for three reasons: (1) Eigen-modes of standing MHD waves provide a natural mechanism for oscillations with a strictly regular period; (2) the period range of $P \approx 0.5 - 5$ s was expected for the MHD fast sausage mode under coronal conditions, while other MHD oscillations modes have significantly longer periods; and (3) the MHD fast sausage mode modulates the loop density, magnetic field strength, and related radio emission (plasma emission or gyrosynchrotron emission), while the MHD kink mode does not modulate the loop density in first order. In addition we might add a forth reason which has not been appreciated previously: These events listed in Table 1 were generally reported to occur during flares, which explains the high densities that are expected on theoretical grounds (due to the sausage mode wave number cutoff criterion $k_c > k$, see Eq. 7), which does not occur for the MHD kink mode.

Because the loop density plays a critical role for MHD fast sausage mode oscillations (Eq. 7), we listed in Table 1 only observations that have information on the period P as well on the electron density n_0 of the oscillating loops. There are only two observations with direct electron density measurements, using soft X-ray emission measures and constraints from the microwave spectrum, which report electron densities of $n_0 = 4.5 \times 10^{10} \text{ cm}^{-3}$ (Asai et al. 2001) and $n_0 = 10^{11} \text{ cm}^{-3}$ (Melnikov et al. 2002). However, we might also extract information on the electron density from any radio burst that is produced by an emission mechanism near the plasma frequency, since the plasma frequency depends only on the electron density n_0 ,

$$\nu_p = 8980 \sqrt{n_0 [\text{cm}^{-3}]} \quad [\text{Hz}] . \quad (12)$$

Plasma emission is the dominant emission mechanism for metric and decimetric radio bursts up to frequencies of $\nu \lesssim 1.5$ GHz, while free-free emission, gyroresonance, and gyrosynchrotron emission dominate at higher frequencies (e.g., see Dulk 1985). A cursory look at Table 1 shows that most of the reported oscillations fall in the frequency range of $\nu \approx 100 - 1000$ MHz, so this corresponds to electron densities of $n_e \approx 10^8 - 10^{10} \text{ cm}^{-3}$ in the case of plasma emission. In Fig. 3 we display the observed oscillation periods P as function of the observed radio frequency ν .

The observed radio frequency uniquely constrains the density n_0 of the oscillating loop segment, for the case of plasma emission. In order to estimate the external density n_e we can use a standard model of the average background corona, for instance the Baumbach-Allen model, which as function of the normalized

height $R = (1 + h/R_\odot)$ is,

$$n_e(h) = 10^8 \left[\frac{2.99}{R^{16}} + \frac{1.55}{R^6} + \frac{0.036}{R^{1.5}} \right] \approx \frac{4 \times 10^8}{R^9} \quad [\text{cm}^{-3}] \quad (13)$$

where the approximation on the right-hand-side holds for $h \lesssim R_\odot/2$. This density model $n_e(h)$ is shown in Fig. 4 (top). Assuming that the fattest possible loops have a width-to-length ratio of $q_w \approx 1/4$, the minimum required density ratio is $n_{0,min}(h)/n_e(h) = 2.4/q_w^2 \approx 40$ (Eq. 7) for loops oscillating in the MHD fast sausage mode due to the long-wavelength cutoff criterion (Eq. 5). This cutoff criterion implies the constraint that physical solutions are only possible for heights $h \gtrsim 40$ Mm, for oscillations observed in the plasma frequency range of $\nu_p \lesssim 1$ GHz (grey area in Fig. 4 top). The two events observed by Asai et al. (2001) and Melnikov et al. (2002) do not fall in this range, because their density is higher and would correspond to plasma frequencies of $\nu_p = 2$ and 3 GHz. The important conclusion that follows, based on the two assumptions that the Baumbach-Allen model represents a realistic density model of the background corona and that oscillating loops are not fatter than a quarter of their length, is that physical solutions for the MHD fast sausage mode are only possible for coronal heights of $h \gtrsim 40$ Mm in the observed frequency range of $\nu \lesssim 1$ GHz, where most of the fast oscillations have been observed (Fig. 3).

Next we investigate the constraints introduced by the pulse periods, which are found in the range of $P_{saus} \approx 0.5 - 5.0$ s (Fig. 3). Denoting the length of the loop segment that participates in the MHD fast sausage mode oscillation with $\lambda/2$, we obtain an upper limit from the phase speed at the wavenumber cutoff k_c (Eqs. 9, 11),

$$\frac{\lambda}{2} = \frac{P_{saus}}{2} v_{ph}(k) \leq \frac{P_{saus}}{2} v_{Ae} , \quad (14)$$

where the Alfvénic speed v_{Ae} is given by the background density model $n_e(h)$ (Eq. 13),

$$v_{Ae}(h) = \frac{B}{\sqrt{4\pi\rho_0}} = \frac{B}{\sqrt{4\pi\mu m_H n_e(h)}} \approx 1210 \left(\frac{B}{20 \text{ G}} \right) \left(\frac{n_e(h)}{10^9 \text{ cm}^{-3}} \right)^{-1/2} \quad [\text{km/s}] , \quad (15)$$

where we used a mean molecular weight of $\mu = 1.3$ for the H:He=10:1 coronal abundance. We plot the sausage mode period P_{saus} as function of the wavelength $\lambda/2$ in Fig. 4 (bottom), for a mean coronal magnetic field of $B = 20$ G (solid line), as well as for a factor of 2 smaller or larger values ($B = 10 - 40$ G). We find that the corresponding wavelength of the oscillating loop segments have values in the range of $0.3 \text{ Mm} < \lambda/2 < 10 \text{ Mm}$ (gray area in Fig. 4 bottom) for pulse periods of $0.5 < P_{saus} < 5.0$ s, which is much smaller than the full loop length ($l = \pi h > 120$ Mm, see gray area in Fig. 4 top) required for the fundamental sausage mode. Because physical solutions are only possible in heights $h > 40$ Mm, the oscillating loop segment has to be located near the top of the loop. Thus we conclude that only a small segment of the loop is oscillating in the MHD sausage mode. Such small oscillating loop segments require wavelengths that correspond to higher harmonics N of the fast sausage MHD mode,

$$\lambda = \frac{2\pi}{k} = \frac{2l}{N} , \quad (16)$$

while lower harmonics cannot oscillate due to the wave number cutoff. The situation is illustrated for the case $N = 3$ in Fig. 5: For instance, if the cutoff is $k \geq k_c = 6\pi/l$, only wavelengths with $\lambda = 2\pi/k \leq 2\pi/k_c = l/3$ are able to oscillate, which is most likely to occur at the loop top where the density contrast and wavelength match the sausage wavenumber cutoff criterion. Alternatively, oscillations at a higher harmonic could occur along the entire loop, but favorable conditions for detection could be restricted to certain segments only (e.g., due to line-of-sight angles or absorption of plasma emission).

An alternative interpretation of these fast radio pulsations in the decimetric range could be made in terms of propagating fast sausage mode MHD waves, where the wavelength is not prescribed by the loop length, but independently by the driver. This interpretation has been proposed in Roberts et al. (1984). However, if this would be the case, the radio dynamic spectra should show parallel drifting bands of emission for every propagating node. Such decimetric burst types have indeed been observed and are called *decimetric fiber bursts* (e.g., Rosenberg 1972; Bernold 1980; Slottje 1981), but many of the observations listed in Table 1 show narrowband pulsations without parallel drifting bands, and thus are not consistent with (impulsively generated) propagating fast sausage MHD waves.

Note that the measurements of Asai et al. (2001) and Melnikov et al. (2002) have longer periods and higher densities than all decimetric observations listed in Table 1, and thus actually allow for global sausage mode oscillations of the entire loop length, for reasonable magnetic fields in the order of $B \approx 40$ G (marked with crosses in Fig. 4 bottom).

4. CONCLUSIONS

This study leads us to the following conclusions:

1. Only the two imaging observations of fast oscillation events ($P \approx 10$ s) by Asai et al. (2001) and Melnikov et al. (2002) are consistent with global MHD fast sausage mode oscillations, satisfying the relation between period and loop lengths as well as the wave number cutoff criterion for the fundamental sausage mode. The required magnetic field is of the order of $B \approx 40$ G.
2. All earlier radio observations of fast oscillation events, which have been reported in the frequency range of $\nu = 100$ MHz – 1 GHz and with periods of $P \approx 0.5 - 5.0$ s, imply for reasonable coronal magnetic field strengths ($B \approx 10 - 40$ G) that the length of the loop segments participating in the MHD fast sausage mode oscillation is much smaller ($\lambda/2 \lesssim 10$ Mm) than the full loop length ($l \approx 100 - 500$ Mm). The sausage mode oscillation seems to be confined to segments where the largest density contrast to the background occurs, most likely near the loop top, in a segment corresponding to a higher harmonic node (see Fig. 5).
3. The wave number cutoff criterion seems to introduce a bimodality of MHD fast mode sausage oscillation phenomena: (1) partial loop oscillations confined to loop segments ($\lambda/2 \ll l$) of high harmonic ($N \gg 1$) nodes for low-density ($n_e \lesssim 10^{10} \text{ cm}^{-3}$) loops that are observable at the plasma frequency in the metric/decimetric frequency range ($\nu \lesssim 1$ GHz); and (2) global loop oscillations ($\lambda/2 = l$) at the fundamental mode ($N = 1$) for high-density ($n_e \approx 10^{10} - 10^{11} \text{ cm}^{-3}$) loops that are observable in soft X-rays and via gyrosynchrotron emission in microwaves.

In this study we explored the diagnostic of MHD fast sausage mode oscillations. It is important to notice that the observed period does not provide a diagnostic of the Alfvénic travel time across the loop diameter ($P = 2.62a/v_A$), as it was commonly believed, but rather provides a lower limit of this quantity (Nakariakov et al. 2003). Moreover, the new finding that fast periods are likely to be caused by oscillations of partial loop segments (at higher harmonic nodes), implies that the magnetic field B cannot be determined by the loop diameter and sausage mode period, unless the harmonic number can be constrained from imaging observations. This study illustrates specific constraints that are contingent on the sausage wave number cutoff, which have been ignored in previous studies.

Acknowledgements:

MJA was partially supported by NASA contract NAS5-38099 (TRACE), VFM was supported by RFBR grant No.02-02-39005 and NSF grant AST-0307670.

References

- Abrami,A. 1970, Solar Phys., 11, 104.
- Abrami,A. 1972, Nature 238/80, 25.
- Achong,A. 1974, Solar Phys., 37, 477-482.
- Asai,A., Shimojo, M., Isobe, H., Morimoto, T., Yokoyama, T., Shibasaki, K., and Nakajima, H. 2001, ApJ 562, L103.
- Aschwanden,M.J. 1986, Solar Phys., 104, 57-65.
- Aschwanden,M.J. & Benz,A.O. 1986, AA, 158, 102-112.
- Aschwanden,M.J. 1987b, *Pulsations of the radio emission of the solar corona. Analysis of observations and theory of the pulsating electron-cyclotron maser*, PhD Thesis, ETH Zurich, pp.1-173.
- Aschwanden,M.J., Bastian,T.S. & Gary, D.E., 1992c, *Bull.Amer.Astron.Soc.* 24/2, 802.
- Aschwanden,M.J., Benz,A.O., & Montello,M. 1994a, ApJ, 431, 432-449.
- Aschwanden,M.J., Benz,A.O. Dennis,B.R. & Kundu,M.R. 1994b, ApJS, 90, 631-636.
- Aschwanden,M.J., Fletcher,L., Schrijver,C., and Alexander,D., 1999, ApJ, , 520, 880.
- Aschwanden,M.J., DePontieu,B., Schrijver,C.J., and Title,A. 2002, Solar Phys., 206, 99.
- Aschwanden,M.J., Nightingale,R.W., Andries,J., Goossens,M., and Van Doorselaere,T. 2003, ApJ, subm.
- Aurass,H., Chernov,G.P., Karlicky,M., Kurths,J., & Mann,G. 1987, Solar Phys., 112, 347-357.
- Bernold,T.E.X. 1980, AAS 42, 43-58.
- Chernov,G.P. & Kurths,J 1990, Sov. Astron. 34(5), 516-522.
- Chernov,G.P., Markeev,A.K., Poquerusse,M., Bougeret,J.L., Klein,K.L. Mann,G., Aurass,H., & Aschwanden,M.J. 1998, AA, 334, 314-324.
- DeGroot,T. 1970, Solar Phys., 14, 176.
- Dröge,F. 1967, Zeitschr.Astrophys. 66, 200.
- Dulk,G.A. 1985, Annu. Rev. Astron. Astrophys. 23, 169.
- Edwin,P.M. and Roberts,B. 1983, Solar Phys., 88, 179.
- Elgaroy,Ø. 1980, AA, 82, 308-313.
- Gotwols,B.L. 1972, Solar Phys., 25, 232-236.
- Kai,K. & Takayanagi,A. 1973, Solar Phys., 29, 461-475.

- Kliem, B., Karlicky, M., & Benz, A.O. 2000, AA, 360, 715-728.
- Kurths, J. & Herzel, H. 1986, Solar Phys., 107, 39-45.
- Kurths, J. & Karlicky, M. 1989, Solar Phys., 119, 399-411.
- Kurths, J., Benz, A.O., & Aschwanden, M.J. 1991, AA, 248, 270-276.
- McLean, D.J., Sheridan, K.V., Steward, R.T., & Wild, J.P. 1971, Nature 234, 140-142.
- McLean, D.J. & Sheridan, K.V. 1973, Solar Phys., 32, 485-489.
- Melnikov, V.F., Reznikova, V.E., & Shibasaki, K. 2002, in Proc. of intern. Conf. *Active Processes on the Sun and Stars*, (eds. Zaitsev, V.V. and Yasnov, L.V., p.225.
- Nakariakov, V.M., Ofman, L., DeLuca, E., Roberts, B., Davila, J.M. 1999, Science 285, 862.
- Nakariakov, V.M. & Ofman, L. 2001, AA, 372, L53.
- Nakariakov, V.M., Melnikov, V.F., and Reznikova, V.E. 2003, AA, , subm.
- Ofman, L. and Wang, T.J. 2002, ApJ, 580, L85.
- Pick, M. & Trottet, G. 1978, Solar Phys., 60, 353-359.
- Roberts, B., Edwin, P.M., and Benz, A.O. 1984, ApJ, 279, 857.
- Rosenberg, H. 1970, AA, 9, 159.
- Rosenberg, H. 1972, Solar Phys., 25, 188-196.
- Sastry, Ch.V., Krishan, V., & Subramanian, K.R. 1981, J. Astrophys. Astron. 2, 59-65.
- Slottje, C. 1981, *Atlas of fine structures of dynamic spectra of solar type IV-dm and some type II radio bursts*, Dwingeloo, The Netherlands.
- Tapping, K.F. 1978, Solar Phys., 59, 145-158.
- Trottet, G., Kerdraon, A., Benz, A.O., & Treumann, R. 1981, AA, 93, 129-135.
- Wang, T.J., Solanki, S.K., Curdt, W., Innes, D.E., and Dammasch, I.E. 2002, ApJ, 574, L101.
- Wiehl, H.J., Benz, A.O., & Aschwanden, M.J. 1985, Solar Phys., 95, 167-179.
- Zaitsev, V.V., Stepanov, A.V., & Chernov, G.P. 1984, Solar Phys., 93, 363-377.
- Zlobec, P., Messerotti, M., Dulk, G.A., & Kucera, T. 1992, Solar Phys., 141 165-180.

Table 1. Observations of oscillations in the period range of $0.5 \text{ s} < P < 1 \text{ min}$ with density information (either from radio frequencies of $\nu < 1.5 \text{ GHz}$ or from soft X-rays emission measures).

Observer	Number of events	Frequency ν [MHz]	Period P [s]	Instrument/ Spatial resolution
Dröge (1967)	> 18	240, 460 MHz	0.2-1.2	Kiel
Rosenberg (1970)	1	220-320 MHz	1.0-3.0	Utrecht
De Groot (1970)	> 25	250-320 MHz	2.2-3.5	Utrecht
Abrami (1970, 1972)	3	239 MHz	1.7-3.1	Trieste
McLean et al. (1971)	1	100-200 MHz	2.5-2.7	Culgoora
Rosenberg (1972)	1	220-320 MHz	0.7-0.8	Utrecht
Gotwols (1972)	1	565-1000 MHz	0.5	Silver Spring
Kai & Takayanagi (1973)	1	160 MHz	<1.0	17' (Nobeyama)
McLean & Sheridan (1973)	1	200-300 MHz	4.28 ± 0.01	Culgoora
Achong (1974)	1	18-28 MHz	4.0	Kingston
Tapping (1978)	14	140 MHz	0.06-5	Cranleigh
Pick & Trottet (1978)	1	169 MHz	0.37, 1.7	5'-7' (Nançay)
Elgaroy (1980)	8	310-340 MHz	1.1	Oslo
Bernold (1980)	> 13	100-1000 MHz	0.5-5	Zurich
Slottje (1981)	> 40	160-320 MHz	0.2-5.5	Dwingeloo
Trottet et al. (1981)	1	140-259 MHz	1.7 ± 0.5	5' (Nançay)
Sastry et al. (1981)	1	25-35 MHz	2-5	30' (Gauribidanur)
Zlobec et al. (1992)	1	333 MHz	9.8-14.2	0.7'-1.5' (VLA)
Zaitsev et al. (1984)	23	45-230 MHz	0.3-5	Izmiran
Wiehl et al. (1985)	1	300-1000 MHz	1-2	Zurich
Aschwanden (1986, 1987b)	10,60	300-1100 MHz	0.4-1.4	Zurich
Aschwanden & Benz (1986)	10	237, 650 MHz	0.5-1.5	Zurich
Kurths & Herzel (1986)	1	480-800 MHz	1.0, 3.5	Tremsdorf
Aurass et al. (1987)	1	234 MHz	0.25-2	Tremsdorf
Kurths & Karlicky (1989)	1	234 MHz	1.3, 1.5	Tremsdorf
Chernov & Kurths (1990)	10	224-245 MHz	0.35-1.3	Izmiran
Kurths et al. (1991)	25	234-914 MHz	0.07-5.0	Zurich
Aschwanden et al. (1992c)	1	1.5 GHz	8.8	0.2'-0.9' (VLA, OVRO)
Aschwanden et al. (1994a,b)	1,1	300-650 MHz	1.15, 1.8	Zurich
Chernov et al. (1998)	1	164-407 MHz	0.2	5'-7' (Nançay)
Kliem et al. (2000)	1	600-2000 MHz	0.5-3.0	Zurich
Asai et al. (2001)	1	17 GHz	6.6	10" (Nobeyama) ^a
Melnikov et al. (2002)	1	17, 34 GHz	8-11, 14-17	10", 5" (Nobeyama) ^b

^aAsai et al. (2001) estimated a loop length of $L = 16 \text{ Mm}$, a loop width of $w = 6 \text{ Mm}$, and a loop density of $n_e = 4.5 \times 10^{10} \text{ cm}^{-3}$, using Nobeyama and Yokoh/SXT data observed during the 1998-Nov-10, 00:12 UT, flare.

^bMelnikov et al. (2002) estimated a loop length of $L = 25 \text{ Mm}$, a loop width of $w = 6 \text{ Mm}$, and a loop density of $n_e = 10^{11} \text{ cm}^{-3}$, using Nobeyama and Yokoh/SXT observed during the 2000-Jan-12, 01:35 UT, flare.

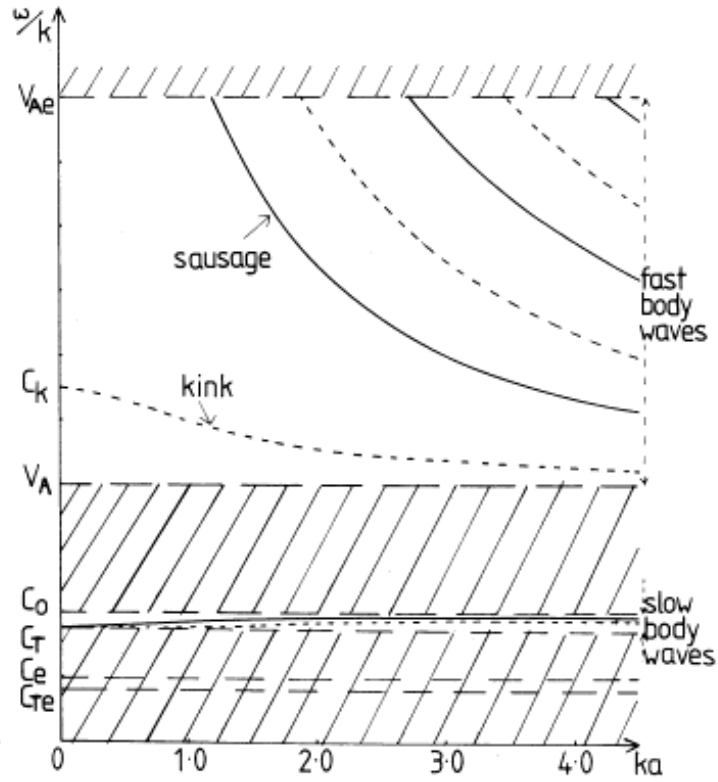


Fig. 1.— The phase speed ω/k is shown for magnetoacoustic waves in a cylindrical fluxtube (with radius a), as function of the longitudinal wave number ka , for coronal conditions $v_{Ae} > v_A > c_t > c_s$. The sausage modes are indicated with solid lines, the kink modes with dashed lines (Edwin & Roberts 1983).

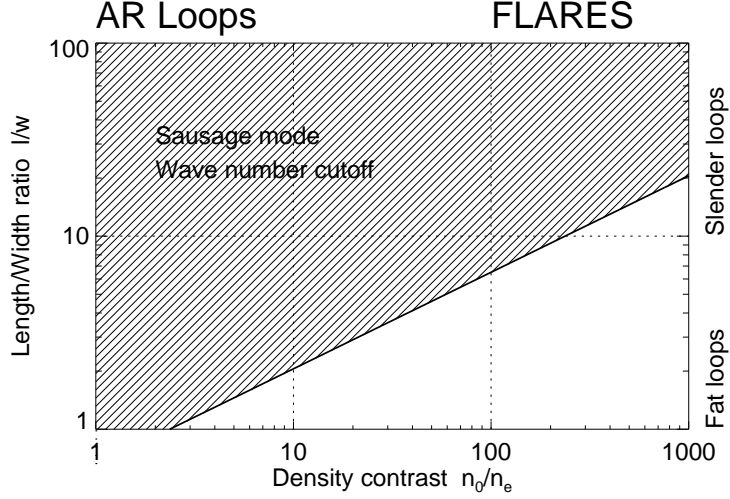


Fig. 2.— The wave number cutoff k_c for sausage mode oscillations expressed as a requirement of the loop length-to-width ratio l/w as function of the density contrast n_0/n_e between the external and internal loop densities (see Eq. 6). Note that sausage mode oscillations in slender loops can occur only for flare conditions.

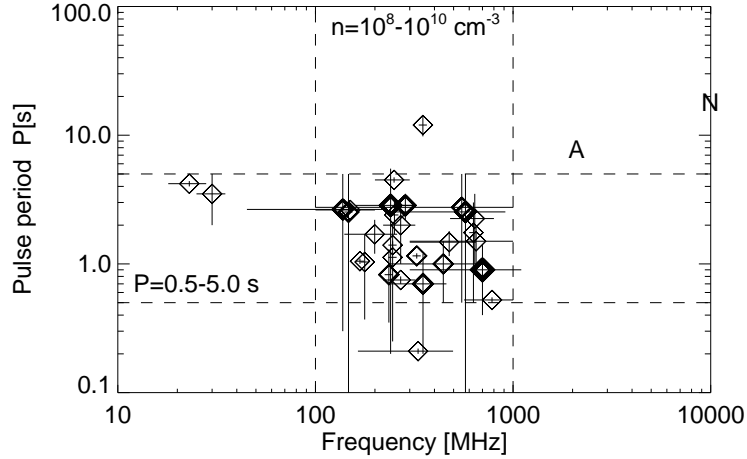


Fig. 3.— Observed oscillation periods as function of the radio frequency, according to the list given in Table 1. Horizontal and vertical bars indicate the ranges in each observation, diamonds the mean values, and thick diamonds label reports on multiple oscillation events. Note that most of the events fall in the range of $P \approx 0.5 - 5.0$ s and $n_0 = 10^8 - 10^{10} \text{ cm}^{-3}$, if one assumes that the radio frequency is near the plasma frequency, $\nu \approx \nu_p$. The letter A and M refer to the observations of Asai et al. (2001) and Melnikov et al. (2003).

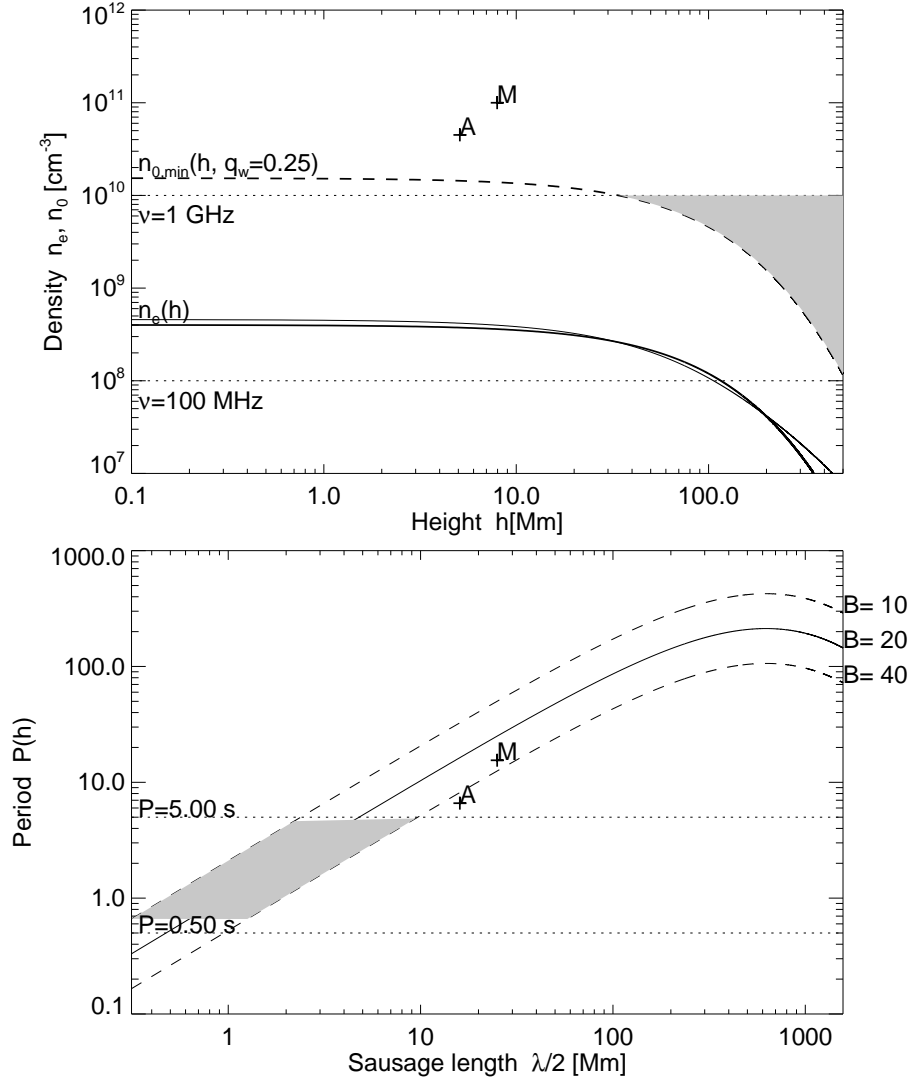


Fig. 4.— *Top*: The Baumbach-Allen density is shown as a model of the average coronal background (thin curve), together with the approximation $n_e(h) \approx 4 \times 10^8 (1 + h/R_\odot)^9$ (thick curve), and the minimum loop density $n_{0,min}(h)$ required for loops that have a width-to-length ratio of $q_w = w/l \leq 0.25$. The height and density range corresponding to a plasma frequency range of 100 MHz-1 GHz is indicated with a grey area. *Bottom*: The MHD fast sausage mode period P_{saus} is shown as function of the sausage length $\lambda/2$ for magnetic fields of $B = 20$ G within a factor of 2. The regime of physical solutions for periods $P = 0.5 - 5$ s and $B = 10 - 40$ G is indicated with a grey area. A and M indicate the values inferred for the observations of Asai et al. (2001) and Melnikov et al. (2002).

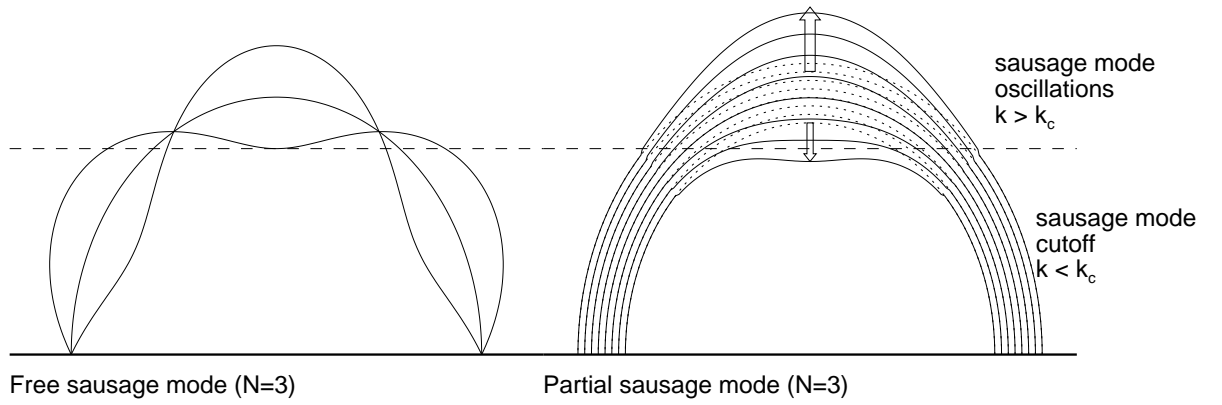


Fig. 5.— Sketch of MHD fast sausage mode oscillation in partial loop segment (right), where the cutoff condition $k > k_c$ is satisfied. For a given width-to-length ratio q_w , oscillations occur in segments where $n_0/n_e > 2.4/q_w^2$ (Eq. 7). The oscillating segment may correspond to a higher harmonic node, e.g., to $N = 3$ here (left).